Di-*n*-butyltin Methyl- and Phenylphosphonates

François Ribot* and Clément Sanchez

Laboratoire de Chimie de la Matière Condensée (UMR CNRS 7574), Tour 54, 5e étage, Université Pierre et Marie Curie, 4 Place Jussieu, F-75252 Paris Cedex 05, France

Monique Biesemans, Frédéric A. G. Mercier, José C. Martins, Marcel Gielen, and Rudolph Willem

High Resolution NMR Centre (HNMR), Free University of Brussels (VUB), Pleinlaan 2, B-1050 Brussel, Belgium

Received February 20, 2001

The structure of $[Bu_2Sn(HO_3PMe)_2]_2$ (**1**), as determined by single-crystal X-ray diffraction, is based on a dimer containing bridging and terminal hydrogenophosphonate ligands. The tin atoms are formally five-coordinate, but exhibit also two additional remote contacts, *d*(Sn−O) ≈ 3.14 Å, which results in a "5+2" type coordination. This crystalline compound and the three other amorphous compounds, $Bu_2Sn(O_3PMe)$ (**2**), $Bu_2Sn(HO_3PPh)_2$ (**3**), and $Bu_2Sn(O_3PPh)$ (**4**), have been characterized by solid state ^{31}P and ^{119}Sn MAS NMR. Compound **1** exhibits a very well resolved ^{31}P MAS NMR spectrum in which three different $^2J(^{31}P-^{119/117}Sn)_{iso}$ scalar couplings can be measured. ^{31}P and ^{119}Sn NMR, $^{31}P-^{19}Sn$ HMQC spectroscopy, and various other 2D NMR techniques at variable temperatures were used to unravel the basic structural unit of compounds **2** and **4** in solution, which is proposed to be based on a trigonal bipyramid of the type R_2SnO_3 with two apical and one equatorial oxygen atom. Compound **1**, in solution, displays a similar local geometry at tin and the same dimeric unit as in the crystalline state. In contrast with **2** and **4**, however, compounds **1** and **3** display an extremely high degree of stereochemical fluxionality based on fast exchange of the bridging and terminal hydrogenophosphonate ligands.

Introduction

Diorganotin carboxylates have been extensively investigated, because of their biological properties[1] as well as their applications in chemistry in general and more specifically in catalysis.[2] They exist as two basic types of compounds depending on the molar ratio $R'COO/R_2Sn$: as dimeric bis(dicarboxylatotetraorganodistannoxane) microclusters of the type $\{[R'COOSnR_2]_2O\}_2$ (I) for a ratio of 1:1 and as monomeric coordination complexes of the type $(R'COO)_2SnR_2$ (II) for a ratio of 2:1.[3,4] Several structural motifs have been observed in the crystalline state for the dimers of type I,[3,4] but only a single one in solution.[4] The compounds of type II have a "4+2" coordination scheme at tin, which exhibits the geometry of a distorted trapezoidal bipyramid.[3,5]

In contrast with tin carboxylates, a much less clear picture on the structural coordination chemistry of organotin phosphonates was developed over the years, despite recent reports on a rich organometallic and inorganic phosphonate chemistry for numerous metals, including tin(II) and tin(IV), which give rise to layered and/or microporous (open-framework) materials,[6−15] molecular cages,[8,16,17] or Langmuir−Blodgett films.[18]

* To whom correspondence should be adressed. E-mail: fri@ccr.jussieu.fr. Fax: (33) 1 44 27 47 69.

(1) (a) Gielen, M.; Lelieveld, P.; de Vos, D.; Willem, R. In *Metal Complexes in Cancer Chemotherapy*; Keppler, B. K., Ed.; VCH: Weinheim, 1993; p 383. (b) Gielen, M. *Coord. Chem. Rev.* **1996**, *151*, 41. (c) de Vos, D.; Willem, R.; Gielen, M.; van Wingerden, K. E.; Nooter, K. *Metal Based Drugs* **1998**, *5*, 179. (d) Clarke, M. J.; Zhu, F.; Frasca, D. R. *Chem. Rev.* **1999**, *99*, 2511.

(2) (a) Smith, P. J., Ed. *Chemistry of Tin*, 2nd ed.; Blackie Academic & Professional: London, 1998. (b) Davies, A. G. *Organotin Chemistry*, VCH: Weinheim, 1997. (c) Mascaretti, O. A.; Furlan, R. L. E. *Aldrichim. Acta* **1997**, *30*, 55. (d) Otera, J. *Chem. Rev.* **1993**, *93*, 1449.

(3) (a) Tiekink, E. R. T. *Appl. Organomet. Chem.* **1991**, *5*, 1. (b) Tiekink, E. R. T. *Trends Organomet. Chem.* **1994**, *1*, 71.

(4) Ribot, F.; Sanchez, C.; Meddour, A.; Gielen, M.; Tiekink, E. R. T.; Biesemans, M.; Willem, R. *J. Organomet. Chem.* **1998**, *552*, 177.

(5) (a) Meriem, A.; Willem, R.; Meunier-Piret, J.; Biesemans, M.; Mahieu, B.; Gielen, M. *Main Group Met. Chem.* **1990**, *13*, 167. (b) Gielen, M.; El Khloufi, A.; Biesemans, M.; Willem, R.; Meunier-Piret, J. *Polyhedron* **1992**, *11*, 1861. (c) Gielen, M.; Bouhdid, A.; Tiekink, E. R. T. *Main Group Met. Chem.* **1995**, *18*, 199. (d) Gielen, M.; Bouâlam, M.; Mahieu, B.; Tiekink, E. R. T. *Appl. Organomet. Chem.* **1994**, *8*, 19.

(6) (a) Clearfield, A. *Prog. Inorg. Chem.* **1998**, *47*, 371. (b) Clearfield, A. *Chem. Mater.* **1998**, *10*, 2801.

(7) (a) Burwell, D. A.; Thompson, M. E. *Chem. Mater.* **1991**, *3*, 14. (b) Burwell, D. A.; Thompson, M. E. *Chem. Mater.* **1991**, *3*, 730. (c) Thompson, M. E. *Chem. Mater.* **1994**, *6*, 1168. (d) Byrd, H.; Cleafield, A.; Poojary, D.; Reis, K. P.; Thompson, M. E. *Chem. Mater.* **1996**, *8*, 2239. (e) Medoukali, D.; Mutin, P. H.; Vioux, A. *J. Mater. Chem.* **1999**, *9*, 2553.

(8) Guerrero, G.; Mutin, P. H.; Vioux, A. *Chem. Mater.* **2000**, *12*, 1268.

(9) (a) Cheetham, A. K.; Férey, G.; Loiseau, T. *Angew. Chem., Int. Ed.* **1999**, *38*, 3268. (b) Bonavia, G.; Haushalter, R. C.; O'Connor, C. J.; Sangregorio, C.; Zubieta, J. *J. Chem. Soc., Chem. Commun.* **1998**, 2187. (c) Finn, R. C.; Zubieta, J. *Inorg. Chem. Commun.* **2000**, *3*, 520. (d) Rodgers, J. A.; Harrison, W. T. A. *J. Chem. Soc., Chem. Commun.* **2000**, 2835.

(10) (a) Massiot, D.; Drumel, S.; Janvier, P.; Bujoli-Doeuff, M.; Bujoli, B. *Chem. Mater.* **1997**, *9*, 6. (b) Bujoli-Doeuff, M.; Evain, M.; Fayon, F.; Alonso, B.; Massiot, D.; Bujoli, B. *Eur. J. Inorg. Chem.* **2000**, 2497.

(11) Corriu, R. J. P.; Leclercq, D.; Mutin, P. H.; Sarlin, L.; Vioux, A. *J. Mater. Chem.* **1998**, *8*, 1827.

(12) Poojary, D. M.; Zhang, B.; Bellinghausen, P.; Clearfield, A. *Inorg. Chem.* **1996**, *35*, 4942.

(13) Jaimez, E.; Bortlum, A.; Hix, G. B.; Garcia, J. R.; Rodriguez, J.; Slade, R. C. T. *J. Chem. Soc., Dalton Trans.* **1996**, 2285.

10.1021/om010140x CCC: $20.00
Publication on Web 05/15/2001

Organotin derivatives that involve phosphates,[19−24] phosphinates,[20,23,25−31] or phosphonates[20,21,23,27,30−48] have been reported in the literature. In many cases the compounds are based on esterified species, and therefore the connecting ability of the phosphorus atom is reduced; for example, a phosphonate monoester or a phosphate diester will mainly result in structural motifs similar to a phosphinate. The following overview on oxyphosphorus organotin derivatives is based on the connectivity patterns of the phosphorus-containing ligands.

Phosphorus atoms with four P−O−Sn links are found in tris(dimethyltin) bis(orthophosphate), $(Me_2Sn)_3(PO_4)_2 \cdot 8H_2O$, which forms infinite ribbons with distorted octahedral geometries at tin.[19] They are also encountered in tris(tributyltin) phosphate, $(Bu_3SnO)_3P{=}O$, which undergoes autoassociation, as suggested by solution NMR experiments, resulting in terminal four- and bridging five-coordinate tin atoms.[20]

Tri- and diorganotin derivatives involving triply bridging phosphorus oxo species are usually described as polymeric compounds where tin atoms exhibit trigonal bipyramidal environments.[20,23,27] The only studies—to the best of our knowledge—on dibutyltinphosphonates with a basic structural unit of the type Bu_2SnO_3PR were made at the end of the 1960s by Ridenour et al.[27a] (R = C_6H_{13}, $CH_2C_6H_5$, C_8H_{17}) and by Freireich et al. (R = C_6H_5).[27b] Triply bridging phenyl phosphates are also found in a tetranuclear methyltin oxo cluster, $\{(MeSn)_2(OH)[O_2P(OPh)_2]_3[O_3P(OPh)]\}_2$.[21]

Potentially doubly bridging phosphorus oxo derivatives (i.e., phosphinates, phosphonate monoesters, or phosphate diesters) generate polymeric compounds with di- and triorganotin structural units.[20,22,23,26−29,34,38,39] In triorganotin derivatives, the tin atom environments generally correspond to trigonal bipyramids, with oxygen atoms in apical positions. Diorganotin derivatives display distorted octahedral geometries at tin, with a C−Sn−C trans configuration. The X-ray structure of $Me_3SnO_2P(OH)Ph$, for instance, shows infinite helicoidal chains.[40] The polymeric structure can also be limited to finite oligomers, as in the triphenyltin derivatives $\{Ph_3Sn[O_2P(OMe)Me]\}_6$[36] and $\{Ph_3Sn[O_2P(OPh)_2]\}_6$,[24] which form only cyclohexamers. When more complex organic moieties are bound to tin, monomeric or dimeric compounds, yet with purely monodentate phosphorus oxo derivatives, can be observed as in the X-ray structure of 1-methyl-5-(*O*-*tert*-butylphosphonic acid)-1-aza-5-stannabicyclo[3.3.0^{1,5}]octane,[45] {5-*tert*-butyl-7-diethoxyphosphonyl-3-ethoxy-3-oxo-1,1-diphenyl-2,3,1-benzoxaphosphastannole,[41] or di-*n*-butyltin pyridine-2-phosphonate-6-carboxylate.[37] In the latter case, the tin atom is seven-coordinate via the addition of a water molecule, corresponding to a pentagonal bipyramid with two apical carbon atoms. Several monoorganotin oxo clusters based on doubly bridging phosphorus oxo derivatives and hexacoordinated tin atoms have also been reported by Holmes and co-workers.[21,25]

A variety of organotin compounds with nonbridging phosphorus oxo derivatives, mainly phosphonate diesters and phosphinate monoesters, have also been reported.[30−33,35,42−44,46−48] Such compounds mostly correspond to adducts on organotin halides, R_nSnX_{4-n} (*n*

(14) Fernandez, S.; Mesa, J. L.; Pizarro, J. L.; Lezama, L.; Arriortua, M. I.; Olazcuaga, R.; Rojo, T. *Chem. Mater.* **2000**, *12*, 2092.
(15) (a) Adair, B.; Natarajan, S.; Cheetham, A. *J. Mater. Chem.* **1998**, *8*, 1477. (b) Stock, N.; Stucky, G. D.; Cheetham, A. *Chem. Commun.* **2000**, 2277. (c) Medeiros, M. E.; Alves, O. L. *J. Mater. Chem.* **1992**, *2*, 1075. (c) Owens, C.; Pytlewski, L. L.; Karyannis, N. M.; Wysoczanski, J.; Labes, M. M. *J. Polym. Sci. B* **1970**, *8*, 81.
(16) (a) Walawalkar, M. G.; Horchler, S.; Dietrich, S.; Chakraborty, D.; Roesky, H. W.; Schäfer, M.; Schmidt, H.-G.; Sheldrick, M.; Murugavel, R. *Organometallics* **1998**, *17*, 2865, and references therein. (b) Walawalkar, M. G.; Roesky, H. W.; Murugavel, R. *Acc. Chem. Res.* **1999**, *32*, 2, 117, and references therein.
(17) (a) Mehring, M. M.; Guerrero, G.; Dahan, F.; Mutin, P. H.; Vioux, A. *Inorg. Chem.* **2000**, *39*, 3325. (b) Guerrero, G.; Mehring, M.; Mutin, P. H.; Dahan, F.; Vioux, A. *J. Chem. Soc., Dalton Trans.* **1999**, 1537. (c) Errington, R. J.; Ridland, J.; Willett, K. J.; Clegg, W.; Coxall, R. A.; Health, S. L. *J. Organomet. Chem.* **1998**, *550*, 473.
(18) Petrushka, M. A.; Talham, D. R. *Langmuir* **2000**, *16*, 5123.
(19) Ashmore, J. P.; Chivers, T.; Kerr, K. A.; Van Roode, J. H. G. *Inorg. Chem.* **1977**, *16*, 191.
(20) Blunden, S. J.; Hill, R.; Gillies, D. G. *J. Organomet. Chem.* **1984**, *270*, 39.
(21) Swamy, K. C. K.; Schmid, C. G.; Day, R. O.; Holmes, R. R. *J. Am. Chem. Soc.* **1990**, *112*, 223.
(22) (a) Kowalski, J.; Chojnowski, J. *J. Organomet. Chem.* **1980**, *193*, 191. (b) Molloy, K. C.; Nasser, F. A. K.; Zuckerman, J. J. *Inorg. Chem.* **1982**, *21*, 1711. (c) Otera, J.; Yano, T.; Kunimoto, E.; Nakata, T. *Organometallics* **1984**, *3*, 426.
(23) Chivers, T.; van Roode, J. H. G., Ruddick, J. N. R.; Sams, J. R. *Can. J. Chem.* **1973**, *51*, 3702.
(24) Molloy, K. C.; Nasser, F. A. K.; Barnes, D.; Van der Helm, D.; Zuckerman, J. J. *Inorg. Chem.* **1982**, *21*, 960.
(25) (a) Holmes, R. R. *Acc. Chem. Res.* **1989**, *22*, 190, and references therein. (b) Day, R. O.; Holmes, J. M.; Chandrasekhar, V.; Holmes, R. R. *J. Am. Chem. Soc.* **1987**, *109*, 9, 940.
(26) Sidibé, M.; Lahlou, M.; Diop, L.; Mahieu, B. *Main. Group Met. Chem.* **1998**, *21*, 605.
(27) (a) Ridenour, R. E.; Flagg, E. E. *J. Organomet. Chem.* **1969**, *16*, 393. (b) Freireich, S.; Gertner, D.; Zilkha, A. *J. Organomet. Chem.* **1970**, *25*, 111.
(28) Shihada, A.-F. *Z. Naturforsch. B Chem. Sci.* **1994**, *49*, 1319.
(29) Shihada, A.-F.; Yousif, H. R. *Z. Naturforsch. B Chem. Sci.* **1991**, *46*, 1568.
(30) Grigoriev, E. V.; Yashina, N. S.; Prischenko, A. A.; Livantsov, M. V.; Petrosyan, V. S.; Pellerito, L.; Schafer, M. J. *Appl. Organomet. Chem.* **1993**, *7*, 353.
(31) Richter, F.; Dargatz, M.; Hartung, H.; Schollmeyer, D.; Weichmann, H. *J. Organomet. Chem.* **1996**, *514*, 233.
(32) Grigoriev, E. V.; Yashina, N. S.; Prischenko, A. A.; Livantsov, M. V.; Petrosyan, V. S.; Massa, W.; Karms, K.; Wocadlo, S.; Pellerito, L. *Appl. Organomet. Chem.* **1995**, *9*, 11.
(33) Mehring, M.; Schürmann, M.; Jurkschat, K. *Organometallics* **1998**, *17*, 1227.
(34) (a) Kellner, K.; Rodewald, L.; Schenzel, K. *Phosphorus, Sulfur Silicon Relat. Elem.* **1991**, *55*, 65. (b) Chaturvedi, A.; Sharma, R. K.; Nagar, P. N.; Rai, A. K. *Phosphorus, Sulfur Silicon Relat. Elem.* **1996**, *112*, 179.
(35) Grigoriev, E. V.; Yashina, N. S.; Petrosyan, V. S.; Pellerito, L.; Gianguzza, A.; Pellerito, A.; Avtomonov, E. V.; Lorberth, J.; Prischenko, A. A.; Livantsov, M. V. *J. Organomet. Chem.* **1999**, *577*, 113.
(36) Masters, J. G.; Nasser, F. A. K.; Hossain, M. B.; Hagen, A. P.; Van der Helm, D.; Zuckerman, J. J. *J. Organomet. Chem.* **1990**, *385*, 39.
(37) Gielen, M.; Dalil, H.; Ghys, L.; Boduszek, B.; Tiekink, E. R. T.; Martins, J. C.; Biesemans, M.; Willem, R. *Organometallics* **1998**, *17*, 4259.
(38) (a) Pandey, J. N.; Srivastava, G. *J. Organomet. Chem.* **1988**, *354*, 301. (b) Nietzschmann, E.; Kellner, K. *Phosphorus, Sulfur Silicon Relat. Elem.* **1991**, *55*, 73.
(39) Cunningham, D.; Kelly, L. A.; Molloy, K. C.; Zuckerman, J. J. *Inorg. Chem.* **1982**, *21*, 1416.
(40) Molloy, K. C.; Hossain, M. B.; Van der Helm, D.; Cunningham, D.; Zuckerman, J. J. *Inorg. Chem.* **1981**, *20*, 2402.
(41) Mehring, M.; Löw, C.; Schürmann, M.; Jurkschat, K. *Eur. J. Inorg. Chem.* **1999**, 887.
(42) Lorberth, J.; Shin, S.-H.; Otto, M.; Wocadlo, S.; Massa, W. *J. Organomet. Chem.* **1991**, *407*, 313.
(43) Freitag, S.; Herbst-Irmer, R.; Richter, F. U.; Weichmann, H. *Acta Crystallogr.* **1994**, *C50*, 1558.
(44) Lorberth, J.; Wocadlo, S.; Massa, W.; Grigoriev, E. V.; Yashina, N. S.; Petrosyan, V. S.; Finocchiaro, P. *J. Organomet. Chem.* **1996**, *510*, 287.
(45) Dakternieks, D.; Jurkschat, K.; Tiekink, E. R. T. *Z. Kristallogr.* **1996**, *211*, 755.
(46) Hartung, H.; Krug, A.; Richter, F.; Weichmann, H. *Z. Anorg. Allg. Chem.* **1993**, *619*, 859.
(47) Kolb, U.; Dräger, M.; Fischer E.; Jurkschat, K. *J. Organomet. Chem.* **1992**, *423*, 339.
(48) Hartung, H.; Krug, A.; Richter, F.; Weichmann, H.; Zeigan, D. *Main Group Metal Chem.* **1994**, *17*, 603.

= 1, 2, 3 and X = Cl or Br), where the coordination of tin is expanded to 5 or 6 by the oxygen atom of the P═O groups. The use of bifunctional nonbridging phosphorus oxo derivatives (e.g., $(EtO)_2P(O)CH(Me)P(O)(OR)_2$)[32] can lead to structures based on chains,[32,44] dimers,[42,43,47] or even monomers.[31,33,35,46] The formation of phosphoryl adducts have also been reported for tetraorganotin derivatives bearing a rigid O,C,O-pincer group of the type (2,6-bis(diethoxyphosphonyl)-4-*tert*-butyl)phenyl.[33] For such cases, the Sn−O contacts generated are weak (2.8−3.0 Å), and the tin coordination is better described as "4+2". On the contrary, the corresponding dichlorotin derivative leads to stronger Sn−O contacts (2.2−2.4 Å) and a six-coordination at tin.[33]

The few data available on diorganotin nonesterified phosphonates,[27] as well as the diversity in the structures and coordination chemistry of organotin phosphonates in crystalline and amorphous states sketched above and the potentials of such derivatives in material sciences illustrated by other metals, prompted us to synthesize and investigate novel di-*n*-butyltin phosphonates, from which a novel structural class emerged. The strategy adopted was based on the well-known chemistry of diorganotincarboxylates,[2−5] in which the molar ratio 1:1 or 1:2 of Bu_2SnO to R′COOH enables one to modulate the structure of the desired compounds. It was expected that varying the molar ratio Bu_2SnO/methyl- or phenylphosphonic acid (1:1 or 1:2 molar ratios) would likewise give rise to a similar structural diversity and contribute to the development of novel diorganotin coordination compounds. However, phosphonates are potentially tridentate dianionic ligands and differences with carboxylates (bidentate and monoanionic) can be expected.

The present work offered us the opportunity to implement and assess the use of ^{31}P-detected 2D HMQC NMR spectroscopy[49] applied to the ^{31}P−^{119}Sn pair, to identify complex $^2J(^{31}P-O-^{119/117}Sn)$ coupling patterns and getting, in this way, insight into possible structures. Several ^{31}P−^{m}Y correlation experiments have been performed with nonmetals, predominantly ^{13}C and ^{15}N.[50] ^{31}P-detected HMQC ^{31}P−^{m}Y pulse sequences have also been used to investigate the structure of silver, platinum, and mercury complexes, as well as of organotungsten, -iron, and -rhodium compounds.[50] However, except for the case of ^{31}P−^{6}Li, correlations between ^{31}P and main group metal nuclei have not been reported.

Results and Discussion

Synthesis. The di-*n*-butyltin derivatives of methyl- and phenylphosphonic acid were synthesized by a method described for carboxylic acids by Davies et al.[51] In a first step, tetra-*n*-butyldi-*n*-propoxydistannoxane, $(n\text{-}Bu_2PrOSn)_2O$, is prepared from di-*n*-butyltin oxide and *n*-propanol in refluxing benzene, under elimination of water. This distannoxane reacts in situ after cooling to room temperature with the phosphonic acid, either in 1:2 or in 1:1 molar ratio, leading to respectively compounds **1** and **2** for the reaction with methylphosphonic acid (H_2O_3PMe) and **3** and **4** for the reaction with phenylphosphonic acid (H_2O_3PPh).

The compounds synthesized were identified by elemental analysis and NMR data to have the empirical formulas $Bu_2Sn(HO_3PMe)_2$ for compound **1**, $Bu_2Sn(O_3PMe)$ for compound **2**, $Bu_2Sn(HO_3PPh)_2$ for compound **3**, and $Bu_2Sn(O_3PPh)$ for compound **4**. Indeed, the FT-IR spectra of compounds **1** and **3** both exhibit two broad vibrations centered at 2370 and around 2820 cm^{-1}. The frequency of the later is ill-defined, as it partially overlaps with the C−H stretching bands. These two broad vibrations are in the ranges for O−H stretching involved in a strong or moderate hydrogen bond, respectively.[52] On the contrary, the FT-IR spectra of compounds **2** and **4** do not show such vibrations.

The compounds **1** and **3** are generated according to

$$4\ H_2O_3P-R + [Bu_2Sn(OPr)]_2O \rightarrow 2\ Bu_2Sn(HO_3P-R)_2 + 2\ PrOH + H_2O$$

whereas compounds **2** and **4** are obtained from the reaction

$$2\ H_2O_3P-R + [Bu_2Sn(OPr)]_2O \rightarrow 2\ Bu_2Sn(O_3P-R) + 2\ PrOH + H_2O$$

The 1:2 compounds **1** and **3** show little to no solubility in most usual organic solvents, except in methanol, where it is anyhow limited (e.g., 1 mg/0.5 mL for **1**). By contrast, the 1:1 compounds **2** and **4** are better soluble in most organic solvents, like chloroform, dichloromethane, benzene, and methanol, up to 60 mg for **2** and 100 mg for **4** in 0.5 mL of dichloromethane or benzene/methanol (1:1 vol.). Tonometry performed on **4** in chloroform, in the concentration domain ranging from 2 to 65 mg of **4** per gram of solvent, reveals a mean molar mass of ca. 5000 ± 100 g/mol, which indicates aggregation in solution. The number of $Bu_2Sn(O_3PPh)$ units per oligomer averages 12.9. The linearity of the tonometry measurements on the explored concentration range suggests the absence of equilibrium between several oligomers of different molar masses. This value of 5000 g/mol is lower than those reported between 10 000 and 7000 g/mol by Freireich et al. on several poly(dibutyltin phenylphosphonate)s which consisted of polymers of the same basic chemical unit, $Bu_2Sn(O_3PPh)$, than **4**.[27b] However, Freireich's polymeric compounds were prepared according to a process differing fairly from ours (different precursors, biphasic media, much shorter times). Moreover, Freireich et al. observed an influence of the synthesis solvent on the molar masses of their polymers.[27b] Ridenour et al. have reported for similar $Bu_2Sn(O_3PR)$ dibutyltinphospho-

(49) (a) Bax, A.; Griffey, R. H.; Hawkins, B. L. *J. Magn. Reson.* **1983**, *55*, 301. (b) Bax, A.; Summers, M. F. *J. Magn. Reson.* **1986**, *67*, 565. (c) Bax, A.; Summers, M. F. *J. Am. Chem. Soc.* **1986**, *108*, 2093. (d) Kayser, F.; Biesemans, M.; Gielen, M.; Willem, R. In *Advanced Applications of NMR to Organometallic Chemistry*; Gielen, M., Willem, R., Wrackmeyer, B., Eds.; John Wiley & Sons: Chichester, 1996; Chapter 3, p 45. (e) Berger, S.; Fäcke, T.; Wagner, R. In *Advanced Applications of NMR to Organometallic Chemistry*; Gielen, M., Willem, R., Wrackmeyer, B., Eds.; John Wiley & Sons: Chichester, 1996; Chapter 2, p 29. (f) Kayser, F.; Biesemans, M.; Gielen, M.; Willem, R. *J. Magn. Reson. A* **1993**, *102*, 249. (g) Martins, J. C.; Biesemans, M.; Willem, R. *Prog. NMR Spectrosc.* **2000**, *36*, 271.

(50) Gudat, D. *Annu. Rep. NMR Spectrosc.* **1999**, *38*, 139.

(51) Davies, A. G.; Kleinschmidt, D. C.; Palan, P. R.; Vasishtha, S. C. *J. Chem. Soc.* **1971**, 3972.

(52) (a) Novak, A. *Struct. Bonding* **1974**, *18*, 177. (b) Hibbert, F.; Emsley, J. *Adv. Phys. Org. Chem.* **1990**, *26*, 255. (c) Bellamy, L. J.; Owen, A. J. *Spectrochim. Acta* **1969**, *25A*, 329. (d) Mikenda, W. *J. Mol. Struct.* **1986**, *147*, 1.

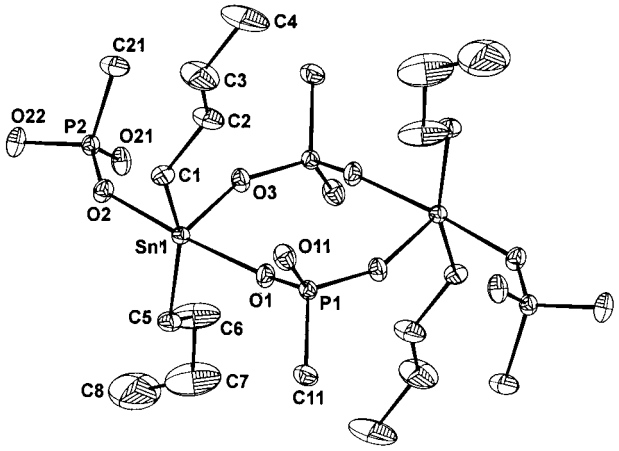

Figure 1. CAMERON[53] drawing of $\{Bu_2Sn(HO_3PMe)_2\}_2$, **1**, showing 30% displacement ellipsoids.

nates (R = C_6H_{13}, $CH_2C_6H_5$, C_8H_{17}) oligomerization degrees ranging from 5 to 37.[27a] Therefore, the molar mass found for compound **4** does not appear contradictory with the results of Freireich et al.,[27b] but mainly indicates that our experimental conditions yield a lighter oligomer.

Crystals suitable for X-ray diffraction analysis could be obtained for compound **1** only, the compounds **2**, **3**, and **4** giving rise to amorphous materials.

Crystalline Structure of 1. The structure of **1**, as determined by X-ray diffraction analysis, is presented in Figures 1 and 2.[53] Selected interatomic distances and bond angles are given in Table 1. The molecular structure of **1** corresponds to a centrosymmetric dimer based on an eight-membered ring containing two five-coordinate tin atoms which exhibit distorted trigonal bipyramid environments (oxygen atoms in apical position, angle O1−Sn1−O2 = 172.1(1)°). One phosphonate group (P1) forms a nonsymmetrical bridge (d(Sn1−O1) = 2.165(4) and d(O1−P1) = 1.498(4), or d(Sn1′−O3′) = 2.058(4) and d(O3′−P1) = 1.512(4) Å). The other one (P2) is formally terminal (d(Sn1−O2) = 2.197(4) and d(O2−P2) = 1.501(4) Å). However, two oxygen atoms (O2 and O22) of this terminal phosphonate form weak contacts (3.099(5) and 3.183(4) Å), nevertheless smaller than the sum of the van der Waals radii (3.70 Å),[54] with a tin atom belonging to a neighboring dimer. These contacts result in the formation of chains of dimers along the *b* axis, such that the coordination of tin is better described as "5+2" (Figure 2). The deviation from the standard trigonal bipyramidal environment is also confirmed by the value of the C1−Sn1−C5 angle, 152.9-(2)°, which is much larger than 120°. A network of hydrogen bonds, associated with an average O−O distance of 2.57 Å, assembles these chains into planes parallel to the *a* and *b* axes (Figure 2). According to the correlation between ν(O−H) and d(OH−O) given by Novak,[52a] this average distance would agree with an O−H stretching of 2370 cm^{-1}, in the strong hydrogen bonds region. Yet, the works of Hibbert et al.[52b] and Bellamy et al.[52c] would correlate such an OH−O distance with an O−H stretching around 2800 cm^{-1}, in the moderate hydrogen bonds region. The FT-IR spectrum of **1** exhibits broad vibrations in both regions, and a more conclusive assignment appears difficult. The acidic hydrogen atoms of the hydrogenophosphonates could not be located on the final difference Fourier map. Yet, according to the hydrogen bonds (Figure 2) and to the lengths of the P−O bonds (Table 1), they are likely located on O11 (for P1) and O22 (for P2).

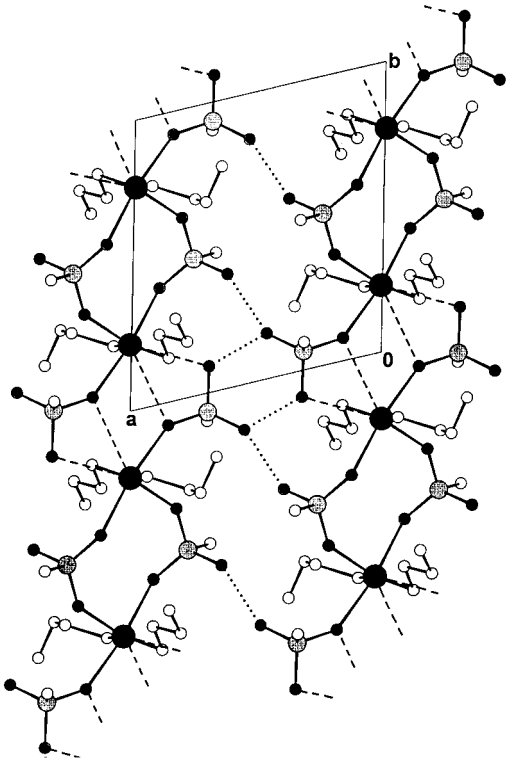

Figure 2. CAMERON[53] drawing of $\{Bu_2Sn(HO_3PMe)_2\}_2$, **1**, showing the long-range organization of the dimers in the plane *ab* (large black circle, Sn; medium gray circle, P; small dark circle, O; and small white circle, C). Hydrogen bonds ($\langle d\rangle$ = 2.57 Å) and weak Sn−O contacts ($\langle d\rangle$ = 3.14 Å) are drawn as dotted and dashed lines, respectively.

Table 1. Selected Interatomic Distances (Å) and Bond Angles (deg) for $\{Bu_2Sn(HO_3PMe)_2\}_2$ (1) with Esd in Parentheses[a]

Sn1−O1	2.165(4)	P1−O1	1.498(4)	P2−O2	1.501(4)
Sn1−O2	2.197(4)	P1−O3′	1.512(4)	P2−O21	1.511(4)
Sn1−O3	2.058(4)	P1−O11	1.564(5)	P2−O22	1.559(4)
Sn1−C1	2.110(5)	P1−C11	1.786(7)	P2−C21	1.779(8)
Sn1−C5	2.107(6)	O21- - -O22*	2.553(6)	O21- - -O11‴	2.587(6)
Sn1- - -O2″	3.183(4)	Sn1- - -O22″	3.099(5)		

O1−Sn1−O2	172.1(1)	O1−P1−O3′	114.7(2)
O1−Sn1−O3	88.4(2)	O1−P1−O11	112.7(3)
O2−Sn1−O3	84.2(2)	O3′−P1−O11	105.7(3)
O1−Sn1−C1	92.8(2)	O1−P1−C11	108.2(3)
O2−Sn1−C1	91.6(2)	O3′−P1−C11	107.8(3)
O3−Sn1−C1	103.0(2)	O11−P1−C11	107.3(3)
O1−Sn1−C5	88.2(2)	O2−P2−O21	116.1(3)
O2−Sn1−C5	90.9(2)	O2−P2−O22	106.3(2)
O3−Sn1−C5	104.1(2)	O21−P2−O22	109.8(2)
C1−Sn1−C5	152.9(2)	O2−P2−C21	108.8(4)
Sn1−O1−P1	153.1(3)	O21−P2−C21	110.0(4)
Sn1−O2−P2	143.2(2)	O22−P2−C21	105.2(4)
Sn1−O3−P1′	142.5(2)		
Sn1−C1−C2	113.0(5)		
Sn1−C5−C6	112.1(5)		

[a] ′ refers to symmetry −*x*, 1−*y*, 1−*z*; ″ refers to symmetry −*x*, −*y*, 1−*z*; ‴ refers to symmetry 1+*x*, *y*, *z*; * refers to symmetry 1−*x*, −*y*, 1−*z*.

Solid State ^{119}Sn and ^{31}P MAS NMR Studies of 1. The $^{31}P\{^1H\}$ MAS NMR spectrum of **1** is presented

(53) (a) Watkin, D. J.; Prout, C. K.; Pearce, L. J. *CAMERON*; Chemical Crystallography Laboratory, University of Oxford: Oxford, U.K., 1996.

Table 2. ^{31}P MAS NMR Data

	δ_{iso} (ppm)	ζ (ppm)	η	σ_{11} (ppm)	σ_{22} (ppm)	σ_{33} (ppm)	intensity (%)	$^2J_{iso}(^{31}P-^{119/117}Sn)$ (Hz)
				$\{Bu_2Sn(HO_3PMe)_2\}_2$ (**1**)				
1X	21.3	−50	0.75	22	−15	−71	50	160
1Y	16.9	50	0.80	−61	−22	32	50	130−215
				$Bu_2Sn(O_3PMe)$ (**2**)				
2X	13.4	−37	0.65	17	−7	−50	100	
				$Bu_2Sn(HO_3PPh)_2$ (**3**)				
3X	13.3	58	0.80	−65	−19	44	49	
3Y	4.5	−62	0.85	52	0	−66	28	
3Y′	3.8	−66	0.85	57	1	−70	22	
				$Bu_2Sn(O_3PPh)$ (**4**)[a]				
4X	3.3						28	
4Y	−0.2						65	
4Z	−4.6						7	

[a] The phosphorus resonances were so broad and strongly overlapping that no attempt to extract the shielding parameters was made.

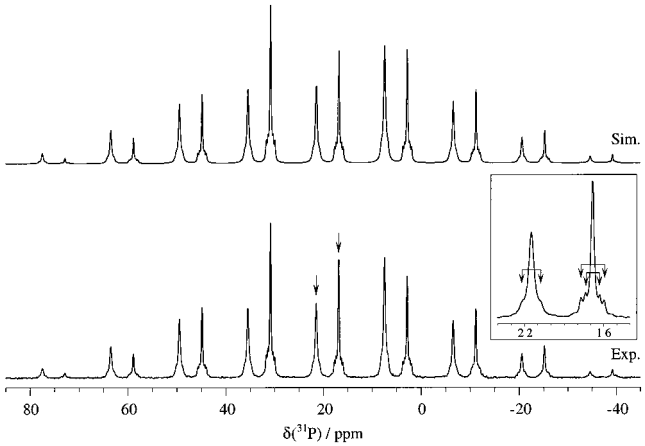

Figure 3. Experimental and simulated ^{31}P MAS NMR spectrum of $\{Bu_2Sn(HO_3PMe)_2\}_2$, **1**, under high-power proton decoupling, $\nu_{MAS} = 1700$ Hz (the isotropic resonances are pointed out with arrows). The inset shows an expansion of the isotropic resonances with the $^2J(^{31}P-^{119/117}Sn)$ satellites pointed out.

in Figure 3. It reveals the existence of two unequivalent sites (1X and 1Y), the NMR characteristics and relative populations of which have been extracted by simulation (Table 2). The two sites are equally populated, in agreement with the X-ray structure. All the resonances (isotropic or spinning sidebands) also exhibit satellites (two pairs for 1Y and one pair for 1X) which can be assigned to unresolved $^2J(^{31}P-^{119/117}Sn)$ scalar couplings. The intensity of each pair of satellites is 16 ± 1% of the corresponding site, indicating that each coupling to the ^{31}P nucleus involves a single tin atom. This feature is in perfect agreement with the molecular structure of **1** as determined from X-ray analysis and enables one to assign unambiguously the low-frequency site (1Y) to the unsymmetrical bridging phosphonate (P1) and the high-frequency site (1X) to the terminal phosphonate (P2). Indeed, P1 is linked to Sn1 and its symmetric Sn1′ through two paths (P1−O1−Sn1 and P1−O3′−Sn1′) of different length, while P2 is linked to Sn1 through a unique path (P2−O2−Sn1). One can note that the main difference between the two phosphorus atom environments is only observed in the O−P−X angles (X = O or C) and not in the P−O and P−C distances ($\Delta d_{max} = 0.004$ Å ≤ esd).

A ^{31}P NMR study on a series of lamelar zinc phosphonates revealed that the $\delta_{iso}(^{31}P)$ moves to high frequency when the phosphonate connectivity increases from a "111" to a "122" type.[10a,55] At first glance, our assignment turns opposite, as the bridging phosphonate (P1), which exhibits a higher connectivity ("011") than the terminal phosphonate (P2, "001"), corresponds to the signal at low frequency. However, if the weak Sn−O contacts (∼3.15 Å) are included in the connectivity analysis, the so-called terminal phosphonate (P2) turns to a "012" connectivity, which is higher than the "011" connectivity of the bridging phosphonate (P1), and our assignment follows the rule found for the zinc phosphonates. This effect of the connectivity on the isotropic chemical shift should anyhow be considered with some care, as it was established for too small a number of compounds, all based on fully deprotonated phosphonates, which is not the case here. Moreover, the same connectivity can lead to fairly different chemical shifts, as observed for some titanium derivatives ($\delta_{iso}(^{31}P) \approx$ 6.5 ppm for the cage compounds $[Ti_4(\mu_3\text{-}O)(OPr^i)_5(\mu\text{-}OPr^i)_3(O_3PPh)_3]$·DMSO and $\delta_{iso}(^{31}P) = -4$ ppm for lamelar $Ti(O_3PPh)_2$, the phosphonate ligands in these compounds being all "111").[8,13,17a]

The asymmetries (Table 2) are close to unity for both types of phosphorus in compound **1**, indicating that local geometries are very far away from 3-fold or higher symmetry, as expected for terminal or bridging hydrogenophosphonates. Such high asymmetries have already been reported for various phosphonic acids and zinc phosphonates which exhibit "112" or "122" connectivities.[10a,55−57] The magnitude of the shielding anisotropies (Table 2) are comparable to values reported for phosphonic acids,[56,57] zirconium carboxyalkylphosphonates,[58] zinc phosphonates, and galium phosphonates.[10] The change of sign of the shielding anisotropies, as observed between sites 1Y (P1) and 1X (P2), has already been observed and arises from the large values

(54) Bondi, A. *J. Phys. Chem.* **1964**, *68*, 441.
(55) The connectivity of a phosphonate is labeled from the number of metal atoms bound to each oxygen; for example, a connectivity noted "111" corresponds to a phosphonate where each oxygen is bound to a single metal, while a connectivity noted "122" corresponds to a phosphonate where one oxygen is bound to a single metal and the two other ones are bound to two metals each.[10a]
(56) (a) Harris, R. K.; Merwin, L. H.; Hägele, G. *J. Chem. Soc., Faraday Trans. 1* **1989**, *85*, 1409. (b) Harris, R. K.; Merwin, L. H.; Hägele, G. *Magn. Res. Chem.* **1989**, *27*, 470.
(57) (a) Klose, G.; Trahms, L.; Möps, A. *Chem. Phys. Lett.* **1985**, *122*, 545. (b) Klose, G.; Möps, A.; Grossmann, G.; Trahms, L. *Chem. Phys. Lett.* **1990**, *175*, 472.
(58) Burwell, D. A.; Valentine, K. G.; Thompson, M. E. *J. Magn. Reson.* **1992**, *97*, 498.

Table 3. ^{119}Sn MAS NMR Data

δ_{iso} (ppm)	ζ (ppm)	η	σ_{11} (ppm)	σ_{22} (ppm)	σ_{33} (ppm)	intensity (%)	coordination
			$\{Bu_2Sn(HO_3PMe)_2\}_2$ (**1**)				
−337.0	825	0.35	−220	69	1160	100	5+2
			$Bu_2Sn(O_3PMe)$ (**2**)				
−276.5	600	0.65	−220	170	880	45	5
−285.0	560	0.80	−220	230	850	55	5
			$Bu_2Sn(HO_3PPh)_2$ (**3**)				
−277.5	770	0.45	−280	60	1050	100	5
			$Bu_2Sn(O_3PPh)$ (**4**)				
−280.0	630	0.70	−255	185	910	100	5

of the asymmetries and from the sorting protocol of the σ_{ii} values established by Haeberlen.[56,59] Two alternative parameters, associated with a different sorting protocol, can be used: the span and the skew.[60] For compound **1**, the spans of both sites turn to be identical, at 93 ppm, and the skews are 0.16 and −0.20 for 1Y (P1) and 1X (P2), respectively. The latter parameter has been found to increase with the phosphonate connectivity in a series of zinc and gallium phosphonates.[10] Yet, according to the nonunivocal connectivity scheme for the phosphonates of compound **1** ("001" vs "012", vide supra), the proposed correlation seems difficult to verify here.

The ^{119}Sn MAS NMR spectrum of **1** shows only one site, in agreement with the X-ray structure (Table 3). The line-width of the resonances (∼1000 Hz) prevents the observation of the multiplicity pattern expected from the $^2J(^{119}Sn-^{31}P)$ couplings. The isotropic resonance (−337 ppm) can be considered as characteristic for a dibutyltin in a "5+2" coordination site. Indeed, the two Sn−O remote contacts (∼3.15 Å, vide supra) have to be taken into account in the shieding of the ^{119}Sn nucleus, as recently evidenced in $\{(BuSn)_{12}O_{14}(OH)_6\}(4\text{-}CH_3C_6H_4\text{-}SO_3)_2\cdot C_4H_8O_2$, where a single tin−oxygen remote contact of about 3.3 Å is able to induce a shielding of about 25 ppm.[61]

Solid State ^{119}Sn and ^{31}P MAS NMR Studies of 2, 3, and 4. The data of the solid state $^{31}P\{^1H\}$ and ^{119}Sn MAS NMR spectra extracted by simulation for the three other compounds, which are all amorphous, are reported in Tables 2 and 3.

The $^{31}P\{^1H\}$ NMR spectrum of compound **3**, which exhibits a Sn:P ratio of 1:2 as **1**, shows three resonances, approximately in a 2:1:1 ratio. The ^{31}P resonances are broader than those of **1** (100 Hz vs 40 Hz), and no $^2J(^{31}P-^{119}Sn)$ coupling satellite could be observed. The two groups of resonances (3X, on one hand, and 3Y and 3Y′, on the other hand) suggest, by comparison with the results obtained for **1** and considering the usual low-frequency shift (ca. 10 ppm) upon methyl to phenyl substitution in phosphonates,[17a] the presence of the two types of phosphonate groups, i.e., bridging (3Y and 3Y′) and terminal (3X). This proposal is supported by the ^{31}P shielding tensor anisotropies and asymmetries (Table 2), which are very similar to those of compound **1**. Here also a sign change occurs between the anisotropies associated with the presumably bridging and terminal phosphonates, yet opposite the case of **1** if the high-frequency site (3X) is considered as terminal.

The $^{31}P\{^1H\}$ MAS NMR spectrum of compound **2** shows only a single broad resonance (450 Hz). The isotropic ^{31}P chemical shift, at lower frequency than the bridging phosphonate of **1**, suggests the existence of phosphonates in which the three oxygens atoms are bound to tin atoms (i.e., connectivity "111" or higher). The presence of such triply bridging phosphonates was previously proposed to explain the polymeric nature of $[Bu_2Sn(O_3PR)]_n$ (R = C_6H_{13}, $CH_2C_6H_5$, C_8H_{17}).[27a] The smaller anisotropy and asymmetry, as compared to **1**, also suggest a different type of phosphonate.

The $^{31}P\{^1H\}$ NMR spectrum of compound **4** is much more complex. Three main broad (300 to 500 Hz) and overlapping resonances, roughly in a 4:9:1 ratio, can be deconvoluted. Because of the spectrum complexity, no ^{31}P shielding tensor parameters could be extracted reliably. The isotropic chemical shifts suggest that two or three oxygen atoms of the various phosphonates are bound to tin atoms. The nonequivalence and the large width of the resonances are in line with the amorphous nature of compound **4**.

The ^{119}Sn MAS NMR spectra of compounds **3** and **4** exhibit a single isotropic resonance, the line-width of which is slightly larger than for **1**. Compound **2** exhibits two overlapping ^{119}Sn isotropic resonances, in a 1:1 ratio, with widths comparable to **1**. These large widths prevent, even more than for **1**, the observation of any $^2J(^{119}Sn-^{31}P)$ scalar coupling splittings. Importantly, the ^{119}Sn isotropic chemical shifts are very similar for the three amorphous solids **2**, **3**, and **4** (ca. −280 ± 5 ppm) but about 60 ppm at higher frequency than for **1**. This last point suggests that the tin environments in compounds **2**, **3**, and **4** are only five-coordinate, the 60 ppm low-frequency shift for **1** being related to the presence of the two additional weak Sn−O contacts found in its structure.[61] The smaller anisotropies and the larger asymmetries also suggest a different coordination, likely smaller at tin than in compound **1**.

Solution State NMR Data of Compounds 1 and 3. The ^{1}H and ^{13}C NMR spectra of compound **1** in CD_3OD display the signals characteristic for a methyl group bound to phosphorus (doublet) and *n*-butyl groups bound to tin, with their relative integrated areas as expected from the molar ratio of the reaction mixture (2 equiv of $CH_3PO(OH)_2$ and 1 equiv of Bu_2SnO). In contrast with the solid state spectrum, the ^{31}P NMR solution spectrum of **1** displays only a single broad resonance at 21.6 ppm, without any $^2J(^{31}P-^{119/117}Sn)$ coupling satellites. This chemical shift is similar to the one found in the solid state for a terminal phosphonate (P2). The coupling splitting is also absent in the ^{119}Sn NMR solution spectrum, which displays a rather sharp resonance at −278 ppm in a 1:1 CD_3OD/C_6D_6 solution, ca. 60 ppm to higher frequency with reference to the solid state ^{119}Sn isotropic chemical shift. In pure CD_3OD, despite the lower solubility, a slight concentration effect on the ^{119}Sn chemical shifts could be observed, ca. 8 ppm to high frequency upon 5-fold dilution. These data, combined with the absence of $^2J(^{31}P-^{119/117}Sn)$ coupling satellites, indicate that the structure observed in the solid state by X-ray crystallography and supported by the solid state NMR data no longer exists as such in

(59) Haeberlen, U. *Adv. Magn. Reson. Suppl. 1* **1976**.
(60) (a) Mason, J. *Solid-State Nucl. Magn. Reson.* **1993**, *2*, 285. (b) Jameson, C. J. *Solid State NMR* **1998**, *11*, 265.
(61) Eychenne-Baron, C.; Ribot, F.; Steunou, N.; Sanchez, C.; Fayon, F.; Biesemans, M.; Martins J. C.; Willem, R. *Organometallics* **2000**, *19*, 1940.

solution and that an intermolecular exchange of the phosphonate moieties fast on the ^{119}Sn and ^{31}P time scales must take place. The latter kind of exchange was already reported earlier for $SnCl_4$, $RSnCl_3$, R_2SnCl_2, and R_3SnCl adducts of the zwitterionic ethyl phosphonate, $EtOPO_2^-CH_2N^+Me_2Et$.[35]

Decreasing the temperature down to 213 K fails to reveal any decoalescence of the resonance toward $^2J(^{31}P-^{119/117}Sn)$ multiplets and satellites in the ^{119}Sn and ^{31}P spectra, respectively, even in the very diluted solution necessarily used because of the very limited solubility of **1** (and **3**). Temperature decrease down to 163 K leads to decoalescence of the single ^{31}P resonance into a major, relatively narrow resonance at 29.5 ppm and several smaller ones between 19 and 23 ppm, however without any $^2J(^{31}P-^{119/117}Sn)$ multiplet decoalescence, showing that the intermolecular exchange of phosphonates is extremely fast, even at the lowest temperatures accessible. The ^{119}Sn resonance shifts, in CD_3OD, from −289 ppm at room temperature to ca. −348 ppm, at 243 K, and simultaneously undergoes a dramatic broadening (from ca. 50 to 400 Hz), leading to a loss of signal-to-noise ratio, followed at lower temperatures by an apparent, ill-defined, decoalescence. Similar observations were made in the ^{119}Sn and ^{31}P NMR spectra of the other $Bu_2Sn(HO_3PR)_2$ compound **3** (R = Ph), the ^{1}H and ^{13}C spectra being as expected.

Solution State NMR Data of Compounds 2 and 4. The ^{1}H NMR spectrum of compound **2** displays a pattern depending on the nature of the solvent. In a $CDCl_3/CD_3OD$ mixture, the resonances are broad, enabling one only to identify the butyl groups and to confirm the ratio of butyl-to-methyl protons expected from the 1:1 $Bu_2SnO:H_2O_3PCH_3$ reaction stoichiometry. One ^{31}P resonance is observed at 13.3 ppm with $^2J(^{31}P-^{119/117}Sn)$ satellites, the intensity of which is in agreement with a phosphorus atom being connected to three tin atoms through Sn−O bridges. The ^{119}Sn NMR spectrum reveals a badly resolved quartet-like resonance at −279 ppm. Both chemical shifts are very similar to the isotropic values found in the solid state. When **2** is (partially) dissolved in C_6D_6 (the undissolved species has the appearance of a transparent gel), the ^{1}H NMR spectrum has sharper lines and reveals the existence of two sets of butyl groups reflecting distinct chemical environments. The ^{13}C NMR spectrum confirms this. The ^{31}P NMR spectrum reveals at least five sharp resonances, centered around 13.4 ppm, with broad tin satellites and superimposed onto a hump resonance. The quartet-like ^{119}Sn resonance at −279 ppm turns out to be an unresolved broad triplet of doublets with $^2J(^{31}P-^{119/117}Sn)$ coupling constants of ca. 160 and 130 Hz.

The phenyl phosphonate analogue, **4**, displays a better solubility in less polar solvents (CD_2Cl_2, $CDCl_3$, and toluene-d_8). All spectra have sharp resonances at room temperature. The ^{31}P NMR spectrum of **4** in CD_2Cl_2, at and below room temperature, shows three major resonances around 1 ppm in the approximate relative ratio of 2:6:5, together with a minor one, all of them being flanked by broad unresolved $^2J(^{31}P-O-^{119/117}Sn)$ coupling satellites (Figure 4). Surprisingly, at 213 K, only a single, slightly broader resonance remains. We attribute this very unusual merging of three resonances

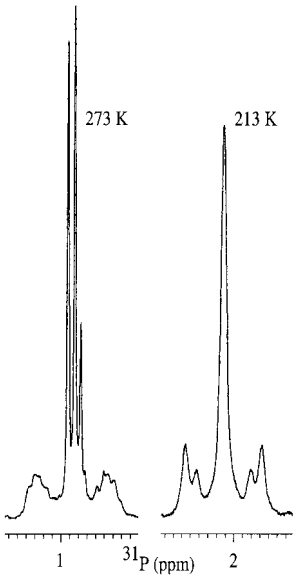

Figure 4. $^{31}P\{^1H\}$ spectrum of compound **4** in CD_2Cl_2 at 213 and 273 K.

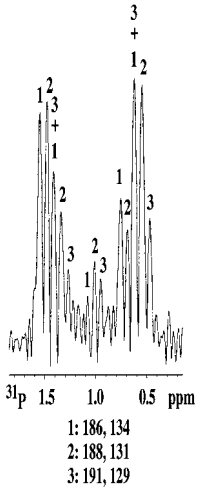

Figure 5. Cross-section along the ^{31}P axis and at the ^{119}Sn resonance frequency of a $^{31}P-^{119}Sn$ HMQC spectrum of compound **4** in CD_2Cl_2. The middle of the pattern shows the residual peaks of the three main ^{31}P resonances (labeled **1**, **2**, **3**), while the side resonances show the $^2J(^{31}P-O-^{119}Sn)$ satellites, with their respective assignment to the main resonance. Each of the three ^{31}P resonance types shows two coupling splittings, with the values indicated below the figure.

at high temperature to a single one at low temperature (a kind of "upside-down" coalescence!) to temperature dependences of the ^{31}P chemical shifts which lead to an accidental isochrony, enhanced by line broadening due to the low temperature. The broad quartet-like pattern of the ^{119}Sn spectrum of **4** around −280 ppm was interpreted as a superposition of three partially unresolved doublets of triplets, originating from a single ^{119}Sn and the three above-mentioned ^{31}P resonances, making use of a 2D $^{31}P-^{119}Sn$ heteronuclear correlation HMQC spectrum (Figure 5).

The $^2J(^{31}P-O-^{119/117}Sn)$ coupling data are given in Table 4, together with all other ^{1}H, ^{13}C, ^{119}Sn, and ^{31}P NMR data. The $^2J(^{31}P-O-^{119}Sn)$ coupling patterns of the $^{31}P-^{119}Sn$ HMQC spectrum (Figure 5) as well as the ^{31}P NMR spectrum at 213 K (Figure 4), where the single

Table 4. ^{1}H, ^{13}C, ^{31}P, and ^{119}Sn NMR Data of Compound 4 at Room Temperature in CD_2Cl_2

	A		B	
butyl groups	^{13}C	^{1}H	^{13}C	^{1}H
α-CH_2	25.9 [746/716][a]	0.73	30.09 [700/666][a]	1.96
			29.92 [718/678][a]	1.93
			29.44 [728/686][a]	1.90
β-CH_2[b]	27.25	1.23	28.03	2.06
	27.21		27.94	
	27.18		27.87	
γ-CH_2	26.9 [113][c]	1.00	27.74 [b]	1.59
			27.68 [b]	
			27.63 [b]	
CH_3	13.6	0.67	14.35	1.14
			14.24	
			14.18	

phenyl group	^{13}C	^{1}H
ipso	136.3 [192][d]	
ortho	131.9 [9][e]	7.65
meta	127.70 [15][f]	7.14
	127.63	
	127.58	
para	130.1	7.31
^{31}P	0.41 [186, 134][g]	
	0.37 [188, 131][g]	
	0.33 [191, 129][g]	
^{119}Sn	−279 (td)[h] [188, 131]	

[a] $^{1}J(^{13}C-^{119/117}Sn)$ coupling constants. [b] Overlapping, no $^{2/3}J(^{13}C-^{119/117}Sn)$ coupling constants visible. [c] Unresolved $^{3}J(^{13}C-^{119/117}Sn)$ coupling constants. [d] $^{1}J(^{13}C-^{31}P)$ coupling constant. [e] $^{2}J(^{13}C-^{31}P)$ coupling constant. [f] $^{3}J(^{13}C-^{31}P)$ coupling constant. [g] $^{2}J(^{31}P-O-^{119}Sn)$ couplings determined from the cross-section at the ^{119}Sn resonance frequency of the 2D ^{31}P-detected $^{31}P-^{119}Sn$ HMQC spectrum. [h] td = triplet of doublets $^{2}J(^{119}Sn-O-^{31}P)$.

resonance with better resolved $^{2}J(^{31}P-O-^{119/117}Sn)$ satellites is observed, reveal that the satellites with the larger value (around 190 Hz) have twice the intensity of those with the smaller value (around 130 Hz). Note the significantly better resolution in the satellite patterns in the $^{31}P-^{119}Sn$ HMQC spectrum (Figure 5), as compared to the standard ^{31}P NMR spectra (Figure 4), which is mainly due to the $^{2}J(^{31}P-O-^{117}Sn)$ satellites in the unresolved $^{2}J(^{31}P-O-^{119/117}Sn)$ satellites of the standard ^{31}P NMR spectra being filtered away in the $^{31}P-^{119}Sn$ HMQC spectrum. The approximate 2:6:5 splitting of the resonances in the ^{31}P spectrum also exists in the ^{13}C NMR spectrum for most of its resonances. The complete assignment of the ^{13}C resonances and the corresponding ^{1}H resonances was achieved by 2D heteronuclear $^{1}H-^{13}C$ HMQC and HMBC experiments, together with a 2D homonuclear ^{1}H TOCSY experiment, which clearly revealed the presence of two "kinds" of butyl groups, given as A and B in Table 4. The α-butyl ^{1}H resonances again reveal a splitting similar to that of the ^{31}P spectrum. Importantly, the relative intensity ratio (2:6:5) of the ^{31}P (and ^{13}C) resonances was found perfectly reproducible for several synthesis batches.

Solution State Bonding Patterns and Structures. The mean molar mass equivalent to 12.9 monomeric $Bu_2Sn(O_3PPh)$ units, combined with the independent data of 2:6:5 demultiplication, also observed in $CDCl_3$, of most ^{31}P, ^{13}C, and even ^{1}H resonances, all these results being obtained in the same concentration range, highly suggests **4** to be a tridecamer, $[Bu_2Sn(O_3PPh)]_{13}$. The alternative, i.e., a mixture of several closely related oligomers, seems less likely, as several attempts of GPC separation of such possible oligomers in compound **4** failed.[62] The impossibility to separate the oligomers could be due to an equlibrium, yet such an equilibrium has to be very slow on the various NMR time scales, since all the nonequivalent ^{31}P and ^{13}C resonances, which appear on a narrow spectral band, and the $^{2}J(^{31}P-O-^{119/117}Sn)$ coupling multiplets or satellites observed are basically uncoalesced at room temperature and even above. Indeed, high-temperature (up to 378 K) ^{31}P NMR in toluene-d_8 shows only appearing and disappearing chemical shift overlappings, but no coalescence phenomenon that would provide us support for the existence of an equlibrium between various oligomers. However, either as a pure tridecamer, which appears most likely, or as a mixture of oligomers, which cannot be totally ruled out, a more precise solution structure cannot be proposed, since no crystal structure determination has been possible for **4** (and **2**, which are both amorphous solids in their isolated state), so no starting point to a solution structure determination is available.

Scheme 1

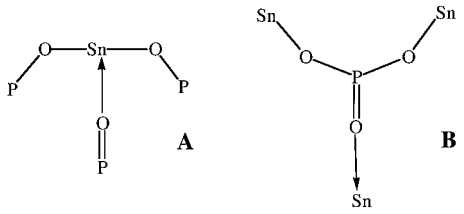

The ^{31}P and ^{119}Sn NMR data at hand, mainly the $^{2}J(^{31}P-O-^{119}Sn)$ coupling multiplet analysis using $^{31}P-^{119}Sn$ HMQC spectroscopy, do enable us, however, to precise at least the local coordination environments of the ^{119}Sn and ^{31}P atoms. The triplet of doublets $^{2}J(^{119}Sn-O-^{31}P)$ coupling pattern in the ^{119}Sn NMR spectrum indicates that each tin atom must be bound to two equivalent (or nearly so) P−O moieties, on one hand, and to a third one with different environment, on the other hand. Similarly, the 2:1 intensity ratio in the $^{2}J(^{31}P-O-^{119/117}Sn)$ coupling satellites flanking the main ^{31}P resonances—especially well visible at low temperature (Figure 4)—indicates that each phosphorus atom must be bound to two equivalent Sn−O moieties, on one hand, and to a third nonequivalent one, on the other hand. The most likely bonding schemes **A** and **B** for Sn and P, respectively, compatible with these patterns, are given in Scheme 1.

At the level of the phosphorus atom, the bonding scheme corresponds to a "111" motif with local C_s symmetry.

The resolved $^{2}J(^{119}Sn-O-^{31}P)$ multiplets, as well as the absence of low-frequency shift in the ^{119}Sn chemical shift around −280 ppm upon temperature decrease and concentration increase, show a very stable structural motif with no tendency to chemical exchange observable on any of the NMR time scales available. The simultaneous presence of the two structural motifs of Scheme 1 is in agreement with the 1P:1Sn stoichiometric ratio of the basic $Bu_2Sn(O_3PR)$ unit of compounds **2** and **4**.

(62) GPC equipment and operating contidions: Pump (Waters 510) and refractometer (Waters RI-410). The columns were μ-styragel (porosity 10^4, 10^3, and 500 Å; grain size 10 μm; length 30 cm). The solvent was THF with a flow rate of 1 mL·min^{-1}; 50 μL of 1 wt % solutions was injected.

A global key observation is that at room temperature all four compounds, the 1P:1Sn compounds **2** and **4** as well as the 2P:1Sn compounds **1** and **3**, exhibit a ^{119}Sn resonance in the same ^{119}Sn chemical shift area around −280 ppm, which strongly suggests that the basic coordination motifs around the tin atom must be very similar, despite the presence of one hydrogen on each phosphonate ligand in compounds **1** and **3** but none in **2** and **4**. On the other hand, the very high similarity of the ^{119}Sn chemical shift of **1** at low temperature and of its ^{119}Sn isotropic chemical shift in the crystalline state, around −350 ppm, lead us to propose that the low-temperature solution structure of **1** mainly consists of the aggregation through "5+2" coordination at the tin atoms of the basic dimeric units also observed in the crystalline state. The ^{119}Sn chemical shift of **1** around −280 ppm is representative of the basic dimeric unit with pure five-coordination at tin, in R_2SnO_3 distorted trigonal bipyramidal configuration, being the dominant species in the dynamic equilibrium at room temperature. Since at low and room temperatures a single averaged ^{119}Sn resonance is observed, the equilibrium between the "5+2" coordinated aggregates of dimeric units and the isolated purely five-coordinate dimers must necessarily be fast on the ^{119}Sn NMR time scale. Such an equilibrium is responsible for the absence of $^2J(^{31}P-^{119/117}Sn)$ splittings, as it causes the phosphonate to move from one tin to another.

The same argument holds for compound **3**. Furthermore, the similar ^{119}Sn chemical shifts, in the same range around −280 ppm, at room temperature strongly suggest an analogous R_2SnO_3 coordination motif for compounds **2** and **4**. Supporting arguments are (i) that the motifs of Scheme 1 proposed from the $^2J(^{119}Sn-O-^{31}P)$ coupling patterns for **4** are compatible with the R_2SnO_3 motif, (ii) that the $^2J(^{119}Sn-O-^{31}P)$ coupling values of **1** in the solid state are in the same value range and obey similar coupling patterns as in **4** in solution, and (iii) that all the $^1J(^{13}C-^{119}Sn)$ coupling values, which range from 700 to 750 Hz, indicate C−Sn−C angles between 138° and 141°, fully compatible with the proposed distorted trigonal bipyramid tin environment.[63] Such a local geometry is similar to the one proposed in the late 1960s by Ridenour et al. from IR and ^{119}Sn Mössbauer data on $[Bu_2Sn(O_3PR)]_n$ (R = C_6H_{13}, $CH_2C_6H_5$, C_8H_{17}).[27a] Finally, the five-coordination of tin implies triply bridging phosphonates for compounds **2** and **4**, but an equal amount of terminal and doubly bridging phosphonates for compounds **1** and **3**, as suggested by ^{31}P MAS NMR and actually proved by X-ray data for **1**.

The only major difference between the compound pairs **2/4** and **1/3** lies in the dramatic contrast between the high stereochemical lability of the latter as opposed to the high stereochemical stability of the former. It is proposed that the key to this difference is the proton bound to the phosphonate ligand in the compound pair **1/3**. Thus, this acidic proton can interact intra- or intermolecularly with oxygens bound to tin atoms and be transferred to them, henceforth destabilizing the O−Sn bonds, as observed. In other terms, this should make an easy electrophilic substitution of tin by the proton on the oxygens of P−O−Sn moieties possible, which results necessarily in a dynamic network of closing and opening O−Sn bonds compatible with the loss of observable $^2J(^{119}Sn-O-^{31}P)$ couplings on both the ^{119}Sn and ^{31}P NMR time scales, as indeed observed. By contrast, the source of stereochemical stability of compound pair **2/4** results from the fact that all three oxygen atoms of a phosphonate ligand are bound to tin atoms and cannot undergo such a substitution.

Noteworthy is that the ^{119}Sn chemical shift of the five-coordinate Bu_2SnO_3 coordination motif, involving phosphonate ligands, appears around −280 ppm, ca. 60−80 ppm to lower frequency, as compared with that of dimeric bis(dicarboxylatotetraorganodistannoxanes) of the type $\{[R'COOSnR_2]_2O\}_2$.[4] This is quite acceptable, considering that a phosphonate contains one oxygen more than a carboxylate ligand and that the phosphorus atom has more electrons and a wider electron cloud than the carboxylate carbon atom. This must result in a higher global shielding of the tin nucleus, conforming to the ^{119}Sn chemical shifts observed at significantly lower frequency.

Experimental Section

Syntheses. Di-*n*-butyltinoxide, Bu_2SnO, $MePO(OH)_2$, and $PhPO(OH)_2$ were purchased from respectively Janssen Chimica (17.936.88), Fluka (64259), and Acros (13079-1000).

Compounds 1 and 2. Di-*n*-butyltin oxide (1.62 g, 6.5 mmol) and an excess (5 mL) of 1-propanol were refluxed in 125 mL of benzene for 4 h. The ternary azeotrope benzene/water/propanol was removed using a Dean Stark funnel. After cooling the reaction mixture to room temperature, a solution of 1.25 g (13 mmol), for **1**, or 0.625 g (6.5 mmol), for **2**, of $MePO(OH)_2$ in a mixture of 20 mL of benzene and 20 mL of methanol was added slowly to the solution. The reaction mixture was stirred at room temperature for 18 h. The reaction mixture was then filtered off, and the solvents were removed from the filtrate under reduced pressure. Only compound **1** could be obtained as a crystalline compound. It was recrystallized from a 1:1 benzene/methanol mixture.

Compound 1. Yield: 65%; mp > 350°. Anal. Found: Sn, 28.8; C, 28.3; H, 6.2; P, 15.8. Calcd for $Sn_2C_{20}H_{52}O_{12}P_4$: Sn, 28.08; C, 28.39; H, 6.21; P, 14.64. NMR (C_6D_6/CD_3OD), chemical shifts in ppm, coupling constants in Hz: ^{1}H: 0.94 (3H, t, CH_3butyl); complex patterns centered at 1.37 (2H, γ-CH_2); 1.54 (2H, α-CH_2, $^2J(^1H-^{119/117}Sn)$ 88); 1.73 (2H, β-CH_2, $^3J(^1H-^{119/117}Sn)$ 106); 1.36 (3H, d, $^2J(^1H-^{31}P)$ 18, CH_3−P). ^{13}C: 13.6 (CH_3 butyl); 27.0 (γ-CH_2, $^3J(^{13}C-^{119/117}Sn)$ 110); 27.4 (β-CH_2, $^2J(^{13}C-^{119/117}Sn)$ 24); 27.7 (α-CH_2, $^1J(^{13}C-^{119/117}Sn)$ 732/701); 13.8 (d, $^1J(^{13}C-^{31}P)$ 144, CH_3−P). ^{31}P: 21.6. ^{119}Sn: −278.

Compound 2. Yield: 64%; mp > 350°. Anal. Found: Sn, 36.7; C, 33.3; H, 6.2; P, 10.4. Calcd for $SnC_9H_{21}O_3P$: Sn, 36.30; C, 33.06; H, 6.49; P, 9.47. NMR ^{1}H ($CDCl_3/CD_3OD$): broad resonances centered at 0.87, 1.29, 1.64 for Bu; 1.29 (3H, d, $^2J(^1H-^{31}P)$ 17, CH_3−P). ^{31}P: 13.3. ^{119}Sn: −279. ^{1}H (C_6D_6): 0.94 (3H, t, CH_3butyl); complex patterns centered at 2.19, 2.06, 1.85, 1.73, 1.41, and 1.23 ppm (butyl CH_2's); 1.36 (3H, d, $^2J(^1H-^{31}P)$ 17.4, CH_3−P). ^{13}C: 14.3 (several overlapping lines, CH_3 butyl); 27.9 (several overlapping broad lines without visible satellites), 27.0, 26.6, 26.0 (butyl CH_2's); 15.0 (d, $^1J(^{13}C-^{31}P)$ 149, CH_3−P). ^{31}P: 13.5, 13.3, 13.0, 12.9. ^{119}Sn: −280 (td, $^2J(^{119}Sn-^{31}P)$ 160 and 130).

Compounds 3 and 4. Di-*n*-butyltin oxide (3.24 g, 13 mmol) and an excess (10 mL) of 1-propanol were refluxed in 250 mL of benzene for 4 h. The ternary azeotrope benzene/water/propanol was removed using a Dean Stark funnel. After cooling the reaction mixture to room temperature, a solution of 4.11 g (26 mmol) for **3**, or 2.05 g (13 mmol) for **4**, of $PhPO(OH)_2$ in

(63) Lockhart, T. P.; Manders, J. J.; Zuckerman, J. J. *J. Am. Chem. Soc.* **1985**, *107*, 4546.

Table 5. Crystallographic Data and Refinement Details for 1

formula	$Sn_2C_{20}H_{52}O_{12}P_4$
M	846.0
cryst color, habit	colorless, ~platelet
cryst size	$0.3 \times 0.3 \times 0.1$ mm^3
cryst syst	triclinic
space group	$P\bar{1}$ (no. 2)
unit cell dimens	$a = 8.612(3)$ Å $b = 9.927(4)$ Å $c = 10.584(6)$ Å $\alpha = 100.37(4)°$ $\beta = 93.94(3)°$ $\gamma = 103.04(3)°$
V	861.4(7) Å^3
Z	1
D_c	1.63 g cm^{-3}
$F(000)$	428
diffractometer	Enraf-Nonius CAD-4
radiation (λ)	Mo Kα (0.71069 Å); graphite monochromator
μ	16.9 cm^{-1}
T	room temperature (22 °C)
scan type	$\omega-2\theta$
scan width	$0.8 + 0.345 \tan(\theta)°$
θ range for data collection	1−30°
hkl ranges	0→ +12; −13 → +13; −14 → +14
no. of reflns collected	5335
no. of unique reflns	5024 ($R_{int} = 0.06$)
abs corr	DIFABS[64] (min. 0.91; max. 1.00)
no. of data/restraints/params	4146 [$I > 3.00\sigma(I)$]/16/174
refinement method	full-matrix least squares on F
secondary extinction param	66
final indices:[a] R, R_w	0.0723; 0.0861
goodness of fit on F	1.075
residual electron density, min./max.	-3.15/+2.89 e Å^{-3}

[a] $R = \sum||F_o| - |F_c||/\sum|F_o|$; $R_w = [\sum(w|F_o - F_c|^2)/\sum(wF_o^2)]^{1/2}$, where $w = w'[1 - (||F_o| - |F_c||/6\sigma(F_o))^2]^2$ and $w' = 1/\sum_r A_r T_r(X)$ with 3 coefficients 7.64, 3.45, and 5.51 for a Chebyshev series, for which X is F_c/F_c (max.).

a mixture of 50 mL of benzene and 50 mL of methanol was added slowly to the solution. The reaction mixture was stirred at room temperature for 18 h. The reaction mixture was then filtered off, and the solvents were removed from the filtrate under reduced pressure.

Compound 3. Yield: 69%; mp 183−185°. Anal. Found: Sn, 21.8; C, 43.8; H, 5.5; P, 12.6. Calcd for $SnC_{20}H_{30}O_6P_2$: Sn, 21.70; C, 43.90; H, 5.54; P, 11.32. ^{1}H (CD_3OD/CCl_4): 0.78 (3H, t,CH_3); 1.20 (2H, m, γ-CH_2); 1.44 (2H, m,α-CH_2); 1.56 (2H, m, β-CH_2); 7.31 (2H, m, meta); 7.42 (1H, m, para); 7.69 (2H, m, ortho). ^{13}C: 14.6 (CH_3); 27.9 (γ-CH_2, $^3J(^{13}C-^{119/117}Sn)$ 112); 28.2 (β-CH_2, $^2J(^{13}C-^{119/117}Sn)$ 23); 29.3 (α-CH_2, $^1J(^{13}C-^{119/117}Sn)$ 700/686); 129.1 (meta, $^3J(^{13}C-^{31}P)$ 14); 132.0 (para); 132.3 (ortho, $^2J(^{13}C-^{31}P)$ 11); 135.2 (ipso, $^1J(^{13}C-^{31}P)$ 190). ^{31}P: 10.4. ^{119}Sn: −275.

Compound 4. Yield: 67%; mp > 350°. Anal. Found: Sn, 28.3; C, 43.0; H, 5.9; P, 8.0. Calcd for $SnC_{14}H_{23}O_3P$: Sn, 30.51; C, 43.22; H, 5.97; P, 7.96. NMR data: see Table 4.

Crystallography. Single crystals of **1** were obtained after cold crystallization of 100 mg of the crude compound in a mixture of 4 mL of C_6H_6 and 4 mL of MeOH. A colorless crystal, suitable for X-ray diffraction, was sealed in a Lindman glass capillary tube, and intensity data were collected at room temperature on an Enraf-Nonius CAD4 diffractometer fitted with graphite-monochromatized Mo Kα radiation ($\lambda = 0.71069$ Å). Details concerning the crystallographic data collection and structure determination are given in Table 5. Cell dimensions were determined from 25 reflections ($17° < \theta < 20°$) dispersed in reciprocal space. Two standard reflections were monitored every hour during data collection and showed a decay of 36%; the data were scaled accordingly. Intensities were corrected for Lorentz and polarization effects, and an empirical absorption correction was applied.[64] The structure was solved using the direct method with the SHELXS program.[65] Successive Fourier maps were used to locate all non-H atoms. The H atoms of the butyl and methyl were placed geometrically at the end of each cycle. A unique isotropic thermal parameter was used for all the H atoms. The H atoms of the hydrogenophosphonate could not be located. Full matrix least-squares refinement, based on F, of atomic parameters, of anisotropic thermal parameters for non-H atoms, and of the unique isotropic thermal parameter for H atoms was carried out with the CRYSTALS programs.[66] The atomic scattering factors were provided by CRYSTALS.[66] Final refinement details are given in Table 5. The numbering scheme employed is shown in Figure 1.

Solid State NMR Experiments. The ^{119}Sn and ^{31}P MAS (magic angle spinning) NMR experiments have been performed on a Bruker MSL300 spectrometer (111.92 and 121.49 MHz for ^{119}Sn and ^{31}P, respectively) equipped with a 4 mm high-speed locked Bruker probe. For ^{119}Sn, the spectral width, pulse durations, and recycling delays were 200 000 Hz (~1800 ppm), 1−1.5 μs (<30°), and 15 s, respectively. Typically, 500−4000 transients were accumulated in order to achieve reasonable signal-to-noise ratios. ^{119}Sn chemical shifts are quoted relative to Me_4Sn, using solid tetracyclohexyltin ($\delta_{iso} = -97.35$ ppm) as a secondary external reference.[67] For ^{31}P, the spectral width, pulse durations, and recycling delays were 30 000 Hz (~250 ppm), 1−2 μs (<30°), and 10−15 s, respectively. A total of 16−400 transients were recorded depending on the sample and spinning rate. High-power proton decoupling was switched on during acquisition to remove the ^{1}H−^{31}P dipolar interaction, which was not fully averaged to zero by the MAS and can dramatically broaden the resonances, especially at low spinning rate. ^{31}P chemical shifts are quoted relative to 85% H_3PO_4, using solid $NH_4(H_2PO_4)$ ($\delta_{iso} = 0.95$ ppm) as a secondary external reference. For both nuclei, at least two experiments, with sufficiently different spinning rates, were run in order to identify the isotropic chemical shifts. The spinning frequencies were stabilized to ±5 Hz.

The ^{119}Sn and ^{31}P spectra were simulated with WINFIT software.[68] The principal components of the shielding tensors were extracted using the Herzfeld and Berger approach.[69] They are reported, following Haeberlen's convention as the isotropic chemical shift ($\delta_{iso} = -\sigma_{iso}$), the anisotropy ($\zeta = \sigma_{33} - \sigma_{iso}$), and the asymmetry ($\eta = |\sigma_{22} - \sigma_{11}|/|\sigma_{33} - \sigma_{iso}|$).[59,70] The accuracy of δ_{iso} corresponds to the digital resolution (±0.5 and ±0.1 ppm for ^{119}Sn and ^{31}P, respectively). The accuracy of ζ was estimated to ±10 and ±4 ppm for ^{119}Sn and ^{31}P, respectively. The accuracy on η is ±0.05.

Solution NMR Experiments. The spectra were recorded at 303 K, unless otherwise stated, on a Bruker AMX500 instrument, equipped with a triple resonance inverse probehead (TBI) with ^{1}H, ^{31}P, or ^{119}Sn and broad band channels, operating at 500.13, 125.76, 202.46, and 186.50 MHz, for ^{1}H, ^{13}C, ^{31}P, and ^{119}Sn, respectively. All 1D spectra and 2D homonuclear ^{1}H TOCSY as well as the 2D heteronuclear ge-^{1}H−^{13}C HMQC and HMBC were obtained from standard pulse programs in the Bruker library. The 2D double heteronuclear ^{31}P−^{119}Sn HMQC spectrum was recorded with ^{31}P detection at 263 K, and the delay for heteronuclear coupling evolution was set at 3.6 ms, with ^{1}H decoupling throughout.

(64) Walker, N.; Stuart, D. *Acta Crystallogr. Sect. A* **1983**, *39*, 158.
(65) Sheldrick, G. M. *SHELXS-86*, Program for Automatic Solution of Crystal Structure; University of Göttingen: Göttingen, Germany, 1986.
(66) Watkin, D. J.; Prout, C. K.; Carruthers, J. R.; Betteridge, P. W. *CRYSTALS issue 10*; Chemical Crystallography Laboratory, University of Oxford: Oxford, U.K., 1996.
(67) Reuter, H.; Sebald, A. *Z. Naturforsch.* **1992**, *48b*, 195.
(68) Massiot, D.; Thiele, H.; Germanus, A. *Bruker Rep.* **1994**, *140*, 43.
(69) Herzfeld, J.; Berger, A. E. *J. Chem. Phys.* **1980**, *73*, 6021.
(70) Harris, R. K.; Lawrence, S. E.; Oh, S. W. *J. Mol. Struct.* **1995**, *347*, 309.

FT-IR Spectroscopy. FT-IR spectra were recorded on a Nicolet Magna-IR 550 spectrometer. Solid samples were dispersed in spectroscopic grade KBr pellets.

Molar Mass Determination by Vapor Pressure Osmometry. The molecular mass measurements were performed with a Knauer vapor pressure osmometer No. 11.00, in chloroform at 43 °C (± 0.01 °C). The calibration was performed with benzil ($C_6H_5COCOC_6H_5$). The accuracy of the determination was estimated from two independent measurements, each being performed with five different concentrations.

Chemical Analyses. Sn, C, H, and P elemental analyses were performed at the "Service Central d'Analyse" in Vernaison (France).

Acknowledgment. The authors thank Dr. J. Vaissermann (Centre de Résolution Structurale, Bat. F-E4, UPMC, Paris, France) for solving the X-ray structure and J. Maquet for her precious assistance in solid state ^{119}Sn and ^{31}P MAS NMR. M.B., R.W., and F.A.G.M. are indebted to the Fund for Scientific Research Flanders (Belgium, grant no. G.0192.98) for financial support. J.C.M. is a Postdoctoral Fellow of the Fund for Scientific Research Flanders (F.W.O.) (Belgium). F.R., C.S., M.B., and R.W. are indebted to the Flemish Ministry of Education and the French Ministries of Foreign Affairs and Education, Research and Technology for the allocation of a Tournesol Grant (no. 99.091).

Supporting Information Available: Further details of the structure determination including bond distances and angles and thermal parameters for $\{Bu_2Sn(HO_3PMe)_2\}_2$, **1**, as well as the ^{31}P MAS NMR spectra of compounds **2**, **3**, and **4** and the ^{119}Sn MAS NMR spectra, with simulations, of compounds **1**, **2**, **3**, and **4**. This material is available free of charge via the Internet at http://pubs.acs.org.

OM010140X